Application of Self Organizing Map Approach to Partial Discharge Pattern Recognition of Cast-Resin Current Transformers

WEN-YEAU CHANG
Department of Electrical Engineering
St. John's University

HONG-TZER YANG *
* Department of Electrical Engineering
* National Cheng Kung University

No. 499, Sec. 4, Tam King Road, Tamsui, Taipei 251, Taiwan
* No. 1, University Road, Tainan City 701, Taiwan
TAIWAN
changwy@mail.sju.edu.tw
* htyang@mail.ncku.edu.tw

Abstract: Partial discharge (PD) measurement and recognition is a significant tool for potential failure diagnosis of a power transformer. This paper proposes the application of self organizing map (SOM) approach to recognize partial discharge patterns of cast-resin current transformer (CRCT). The PD patterns are measured by using a commercial PD detector. A set of features, used as operators, for each PD pattern is extracted through statistical schemes. The proposed SOM classifier has the advantages of high robustness to ambiguous patterns and is useful in recognizing the PD patterns of electrical transformers. To verify the effectiveness of the proposed method, the classifier was verified on 250 sets of field-test PD patterns of CRCTs. The test results show that the proposed approach may achieve quite satisfactory recognition of PD patterns.

Key-Words: Cast-resin current transformer, Partial discharge, Pattern recognition, Self organizing map

1 Introduction

Partial discharge measurement and pattern recognition are important tools for improving the reliability of high-voltage insulation systems. The pattern recognition of PD aims at identifying potential insulation defects from the measured data. The potential defects can then be used for estimating the risk of insulation failure of the high-voltage equipment [1].

In the presence of a sufficiently strong electric field, a sudden local displacement of electrons and ions will lead to a PD if there exists a defect in an insulator [2]. A PD event that occurs in the epoxy resin insulator of high-voltage equipment would have harmful effects on insulation that may finally cause service failure. A defect in high-voltage equipment, resulting in PD, will have a corresponding particular pattern. Therefore, pattern recognition of PD is significant for insulation condition evaluation of high-voltage equipment.

Thanks to physical understanding of PD made substantial progress in the last decade, it can now be exploited to support interpretation of insulation defects [1]. Recently, several methods have been employed for the pattern recognition of PD, including neural networks [3], expert systems, fuzzy classification, and wavelet analysis methods.

The application of neural networks to pattern recognition and system identification has become a major trend in the fault diagnosis. Neural networks has been applied for spatial variability identification of greenhouse [4], and PD pattern recognition of current transformers [5], and PD monitoring technique of gas insulated substation [6]. Although the speed of neural networks allows real-time operation with comparable accuracy, the training process of multilayer neural networks is often very slow, and the training data must be sufficient and compatible.

The recognition of PD pattern and the estimation of insulation performance are relatively complicated, a task which is often completed by experienced experts. Several expert systems for the diagnostics of insulation systems have been developed [7]. The expert system method acquires the knowledge of human expertise to build knowledge base. However, it needs to build and maintain the base with efforts.

The third method is the fuzzy clustering algorithm [8]. The fuzzy c-means clustering algorithm is one of the most popular fuzzy clustering algorithms [9]. Fuzzy c-means clustering algorithm has been applied for pattern recognition for PD of CRCT [10].

Another method is the wavelet analysis method, which has been used to carry out time-frequency

analysis in fault diagnosis [11] and de-noising [12]. Wavelet analysis method has also been applied to identify the PD characteristics by decomposition of acoustic emission signals [13] and PD signal de-noising [14-16].

In this paper, a novel SOM based pattern recognition technique for the PD identification of CRCT is proposed with more effectiveness and robustness than the conventional pattern recognition methods.

This paper is organized as follows. Creation of the PD pattern dataset is described in Section 2. The development of the algorithm of feature extraction is described in Section 3. The principles of SOM and the operation flowchart of the proposed pattern recognition scheme are given subsequently. The experimental results and the analysis using 250 sets of field-test PD patterns from five artificial defect types of CRCTs are presented in Section 5. From the test results, the effectiveness of the proposed scheme to improve the recognition accuracy has been demonstrated. The paper is concluded in the last Section.

2 PD Pattern Dataset Creation

In order to investigate the PD features and to verify the classification capabilities of the SOM for different PD types commonly occurring in CRCTs, a PD dataset is needed. The PD dataset was collected from laboratory tests on a series of model CRCTs. The material and process used to manufacture the model CRCTs were exactly the same as that of making a field CRCT. The specifications of model CRCTs are shown in Table 1. Five types of experimental models with artificial defects embedded were made to produce five common PD events in the CRCTs.

The five PD activities include (a) normal PD activity (NM) in standard CRCT, (b) internal cavity discharge (VH) caused by an air cavity inside the epoxy resin insulator on the high-voltage side, as shown in Fig. 1, (c) internal cavity discharge (VL) caused by two cavities inside the epoxy resin insulator on the low-voltage side, as shown in Fig. 2, (d) internal fissure discharge (FH) caused by an air fissure inside the epoxy resin insulator on the high-voltage side, as shown in Fig. 3, (e) internal discharge (MH) caused by a metal-line impurity inside the epoxy resin insulator on the high-voltage side, as shown in Fig. 4.

The PD events were detected by a PD detecting system set up in our laboratory. The structure of the PD detecting system is shown in Fig. 5. It includes a step-up transformer, capacitor coupling circuit, PD

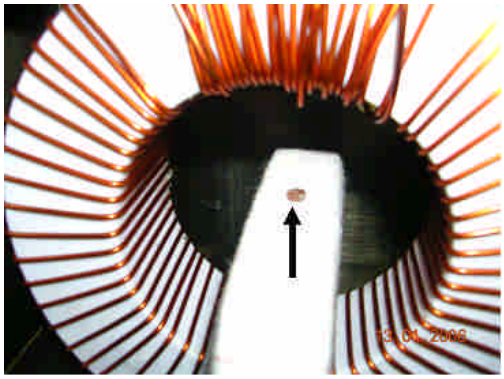

Fig. 1 VH on the high-voltage side of CRCT

Fig. 2 VL on the low-voltage side of CRCT

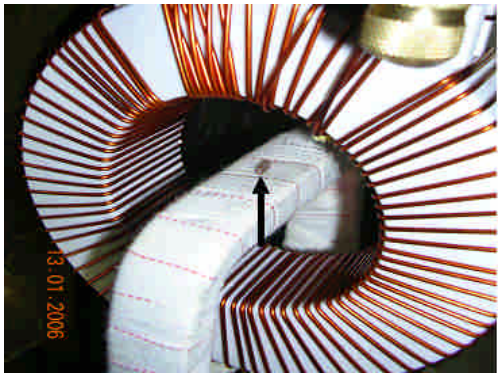

Fig. 3 FH on the high-voltage side of CRCT

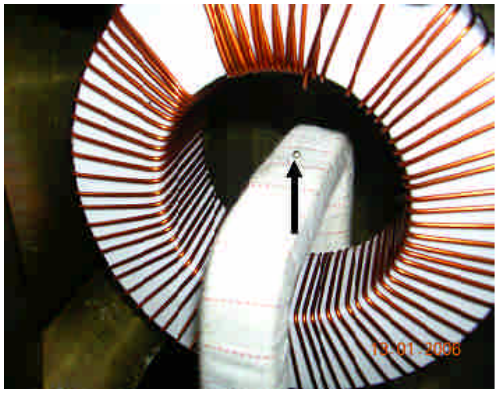

Fig. 4 MH on the high-voltage side of CRCT

Table 1 Specifications of model CRCTs

Service Voltage	Primary Current	Secondary Current	Burden
12000 V	20 A	5 A	40VA

detector, and the CRCT under test. Through the testing processes, all the data measured were digitally converted in order to save them in the computer memory.

Then, the phase-related distributions of PD derived from the original PD data are obtained in relation to the waveform of the field-test high voltage. The high voltage in the field tests is assumed to be held constant and the voltage phase angle is divided into a suitable number of windows (blocks). The PD detector, shown in Fig. 5, is used for acquisition of all the individual quasi-integrated pulses and quantifying each of these PD pulses by their discharge magnitude (q), the corresponding phase angle (ϕ), at which PD pulses occur and the number of discharge (n) over the chosen block. The analysis software (DDX DA3) plots these data as functions of the phase positions [17].

The three phase-related distributions refer to the peak pulse magnitude distribution $H_{qmax}(\phi)$, the average pulse magnitude distribution $H_{qn}(\phi)$, and the number of pulse distribution $H_n(\phi)$. The typical phase-related distributions of PD patterns for the four kinds of defects (VH, VL, FH, and MH) are shown in Figs. 6 to 9, respectively. As shown in Figs. 6 to 9, the PD patterns of deferent defects display discriminative features.

3 Statistical Feature Extraction

Feature extraction is a technique essential in PD pattern recognition to reduce the dimension of the original data. The features are intended to denote the characteristics of different PD statuses [18]. Several statistical methods of feature extraction are described in this section; five statistical operators are extracted from phase-related distributions. Definitions of the operators are described below. The profile of all these discrete distribution functions can be put in a general framework, i.e., $y_i = f(x_i)$ [17].

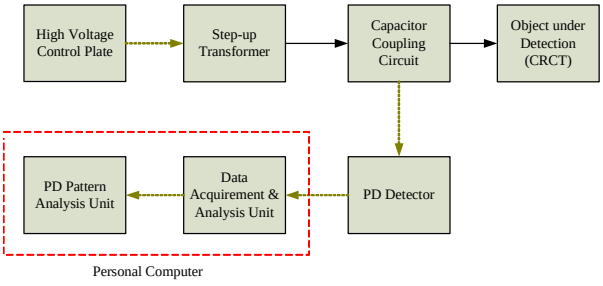

Fig. 5 System configuration of the PD detecting system

The statistical operators of mean (μ) and variance (σ^2) can be computed as follows:

$$\mu = \frac{\sum x_i f(x_i)}{\sum f(x_i)} \quad (1)$$

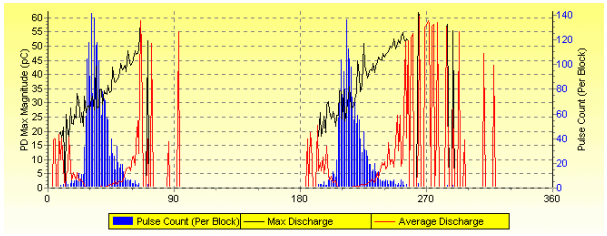

Fig. 6 Typical phase-related distributions of PD for the VH defect

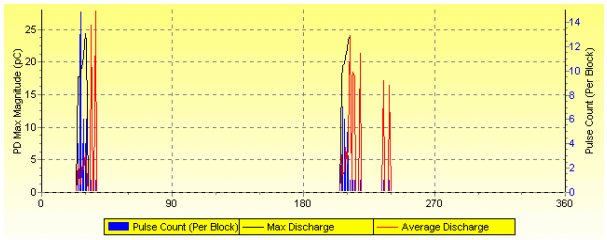

Fig. 7 Typical phase-related distributions of PD for the VL defect

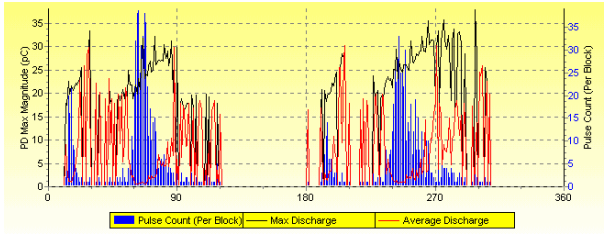

Fig. 8 Typical phase-related distributions of PD for the FH defect

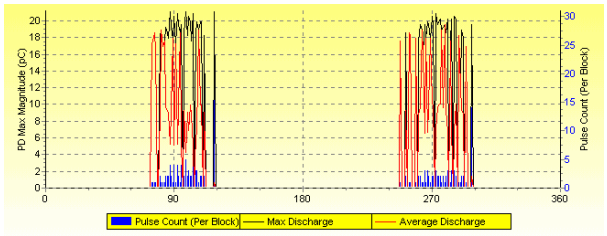

Fig. 9 Typical phase-related distributions of PD for the MH defect

$$\sigma^2 = \frac{\sum (x_i - \mu)^2 f(x_i)}{\sum f(x_i)} \quad (2)$$

Skewness (S_k) is extracted from each phase-related distribution of PD to denote the asymmetry of the distribution. It can be represented as:

$$S_k = \frac{\sum (x_i - \mu)^3 p_i}{\sigma^3} \quad (3)$$

Kurtosis (K_u) is extracted to describe the sharpness of the distribution as:

$$K_u = \frac{\sum (x_i - \mu)^4 p_i}{\sigma^4} - 3 \quad (4)$$

In (1) and (2), x_i is the statistical value in the phase window i, p_i is the related probability of appearance.

Skewness is a measure of asymmetry degree with respect to normal distribution. If the distribution is totally symmetric, then S_k=0; if the distribution is asymmetric to the left of mean, S_k>0; and if it is asymmetric to the right of mean, S_k<0. Kurtosis is an indicator of sharpness of distribution. If the distribution has the same sharpness as a normal distribution, K_u=0; and if it is sharper than normal, K_u>0; and if it is flatter than normal, K_u<0 [17].

Peaks (P_e) count the number of peaks in the positive or negative half of a cycle of the distribution.

Asymmetry (D_a) represents the asymmetrical characteristic of partial pulses in both positive and negative cycles. It is given by:

$$D_a = \frac{N^+ \sum q_i^-}{N^- \sum q_i^+} \quad (5)$$

where N^- is the number of PD pulses in the negative cycle, N^+ is the number of PD pulses in the positive cycle. q_i^- is the amplitude of the PD pulse at a phase window i in the negative cycle, and q_i^+ is the amplitude of the PD pulse at a phase window i in the positive cycle.

The cross correlation factor (C_c) can be expressed as:

$$C_c = \frac{\sum x_i \cdot y_i - \sum x_i \cdot \sum y_i / n}{\sqrt{(\sum x_i^2 - (\sum x_i)^2 / n) \cdot (\sum y_i^2 - (\sum y_i)^2 / n)}} \quad (6)$$

where x_i is the statistical value in the phase window i of the positive half cycle, y_i is the statistical value in the corresponding window of the negative half cycle, and n is the number of phase window per half cycle.

Cross correlation factor indicates the difference in the distribution sharps of both positive and negative half cycles. C_c=1 means the sharps are totally symmetric, C_c=0 means sharps are totally asymmetric.

As S_k, K_u and P_e are applied to both positive and negative cycles of $H_{qmax}(\phi)$, $H_{qn}(\phi)$, and $H_n(\phi)$, a total of 18 features can be extracted from a PD pattern. D_a and C_c are applied to indicate the difference or asymmetry in positive and negative cycles of $H_{qmax}(\phi)$, $H_{qn}(\phi)$, and $H_n(\phi)$, and a total of 6 features can be extracted from a PD pattern. Therefore, after the feature extraction procedure, a feature vector of 24 statistical features is built for each PD pattern.

The typical statistical features extracted by the analysis software (DDX DA3) from PD patterns for the four kinds of defects (VH, VL, FH, and MH) are shown in Figs. 10 to 13, respectively.

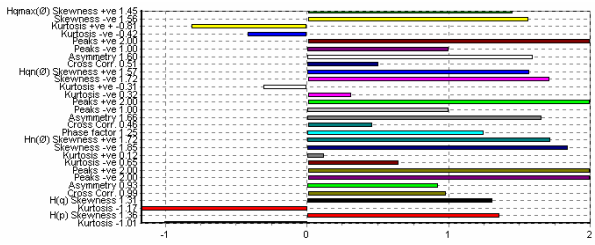

Fig. 10 Typical statistical features of PD for VH

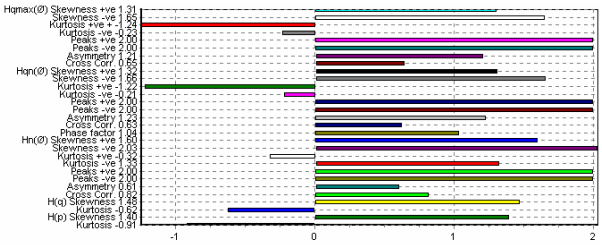

Fig. 11 Typical statistical features of PD for VL

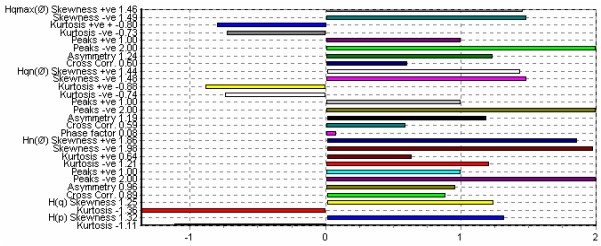

Fig. 12 Typical statistical features of PD for FH

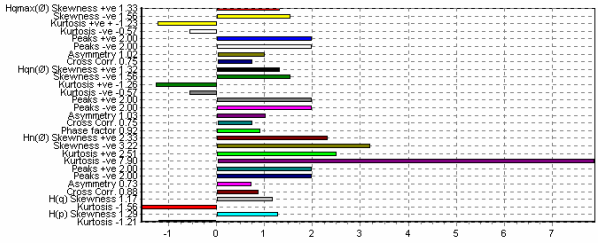

Fig. 13 Typical statistical features of PD for MH

The use of statistical featuring operators for the patterns instead of the distribution profiles can significantly reduce the dimension of the database. To a certain degree, they can characterize the PD patterns with reasonable discrimination [19].

4 SOM-Based PD Pattern Recognition Method

In this section, the algorithms of SOM and SOM-based PD pattern recognition scheme are described. The PD recognition through SOM in multidimensional feature space is also validated on the basis of the laboratory PD dataset as mentioned above.

4.1 SOM Algorithm

The SOM is a typical unsupervised neural network, which maps the multidimensional space onto a two dimensional space by preserving the original order. It simulates the self-organizing feature map's function of the human cerebrum. The SOM is a two-layer neural network that consists of an input layer in a line and an output layer constructed of neurons in a two-dimensional grid as shown in Fig. 14.

The arithmetic of SOM maps random dimension input vectors to one or two-dimension dispersed graphics and maintain its original topologies. With continuous competitive learning, weight vectors would separate from each other in the input space and form one kind of pattern representation. So, SOM learns to recognize groups of similar input vectors in such a way that neurons which are physically close to each other in the neuron layer respond to similar input vectors.

Different from other clustering mapping methods for unsupervised data, mapping relationship of SOM can be highly nonlinear, directly showing the similar input vectors in the source space by points close in the two-dimensional target space [18]. Along with the similarity of the input data, SOM potentially leads to a classification result. It has been applied for PD pattern recognition of turbo-generators [18] and gas insulated switchgear [20], and for power system voltage stability assessment [21].

4.2 SOM-based PD Pattern Recognizing Procedure

The proposed SOM-based PD pattern recognition scheme for CRCTs has been successfully implemented in the PC-based software (MATLAB). The overall operation flowchart is shown in Fig. 15. The procedure of the proposed recognition scheme is described briefly as follows.

Step1 A grid of SOM output layer neurons is set up with initial given weight vectors.
Step2 An input vector is chosen randomly from the input space.
Step3 A winning neuron on the output layer is determined by calculating the Euclidean distance between the input vector and the weight vectors of all neurons in the grid.
Step4 The weight vector of the winner and the weight vectors of its neighbouring neurons are adjusted according to the learning rate.
Step5 Iterate the procedures from Steps 2 to 4 above, till the training process is finished.
Step6 Save the weight vectors of the trained SOM.
Step7 Use the trained SOM to identify the defect types of CRCTs.

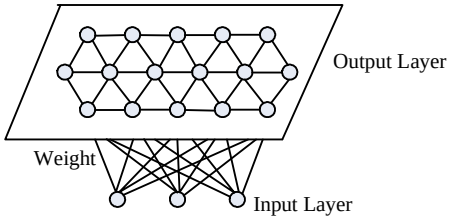

Fig. 14 System structure of SOM

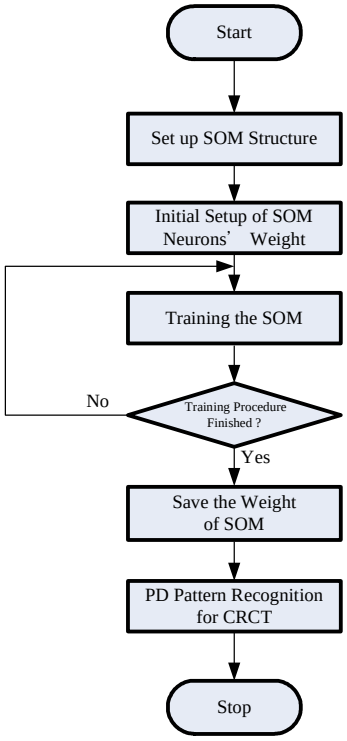

Fig. 15 Flowchart of the SOM-based recognition scheme

5 Experimental Results

To verify the proposed approach, a practical experiment is conducted to demonstrate the effectiveness of the PD pattern recognition scheme. The proposed method has been implemented according to the field-test PD patterns collected from the laboratory. Five types of experimental models with artificial defects are purposely embedded to produce five common PD events in CRCTs.

The proposed method has been implemented according to the field-test PD patterns collected from our laboratory. The input data to a PD recognition system are the peak pulse magnitude distribution $H_{qmax}(\phi)$, the average pulse magnitude distribution $H_{qn}(\phi)$, and the number of pulse distribution $H_n(\phi)$..

Associated with their real defect types, there are a total of 250 sample data for different PD events. Each PD event contains 50 patterns of sample data, of which 30 patterns are training data and 20 patterns are testing data.

The statistical feature extraction methods are used to extract 24 statistical features for each pattern. But, some of the statistical features are futile for pattern recognition. So, the combination of feature vector will influence the accuracy of pattern recognition. In this paper, the selecting index of statistical features is the standard deviation of each feature calculated from the training data. To evaluate the best combination of feature vector, we set up three systems of training sets. In System 1, the feature vector includes 10 features, which have the lower standard deviation. In System 2, the feature vector includes 12 features; and in System 3 the feature vector includes 14 features. Table 2 shows the combination of feature vector for Systems 1 to 3.

In System 1, the number of neurons in the input layer of SOM is designed to comprise the 10 statistical featuring operators mentioned above. The numbers of neurons in input layer of SOM are set to be 12 and 14 for System 2 and System 3, respectively. To evaluate the performance of different structure of SOM, the experimental tests are carried out on 3 types of SOM. The output layer of Type 1 SOM in the three systems is a two-dimensional space comprising 15 by 15 neurons. The output layer of Type 2 SOM in the three systems is a two-dimensional space comprising 17 by 17 neurons. The output layer of Type 3 SOM in the three systems is a two-dimensional space comprising 20 by 20 neurons. The structures of 3 types of SOM are shown in Table 3.

Table 2 Combination of feature vector for 3 systems

System 1						
Distribution	Cycle	S_k	K_u	P_e	D_a	C_c
$H_{qmax}(\phi)$	Positive		●		●	●
	Negative	●				
$H_{qn}(\phi)$	Positive		●		●	
	Negative	●				
$H_n(\phi)$	Positive		●		●	
	Negative	●				
System 2						
Distribution	Cycle	S_k	K_u	P_e	D_a	C_c
$H_{qmax}(\phi)$	Positive		●		●	●
	Negative	●				
$H_{qn}(\phi)$	Positive		●		●	
	Negative	●	●			
$H_n(\phi)$	Positive	●	●		●	
	Negative	●				
System 3						
Distribution	Cycle	S_k	K_u	P_e	D_a	C_c
$H_{qmax}(\phi)$	Positive	●	●		●	●
	Negative	●				
$H_{qn}(\phi)$	Positive		●		●	●
	Negative	●	●			
$H_n(\phi)$	Positive	●	●		●	
	Negative	●				

●: selected feature

Table 3 The structures of 3 types of SOM

SOM	System	Neurons in Input layer	Neurons in Output layer
Type 1	System 1	10	15×15
	System 2	12	15×15
	System 3	14	15×15
Type 2	System 1	10	17×17
	System 2	12	17×17
	System 3	14	17×17
Type 3	System 1	10	20×20
	System 2	12	20×20
	System 3	14	20×20

The training data consist of 150 patterns, which were randomly chosen from the 250 sets of sample data. The other 100 patterns were used as the testing data. After the training process, the weight vectors of the trained SOM were saved.

To verify the training effectiveness of the SOM, training data are applied to the SOM again. Tables 4 to 6 show the test results of the training data for Types 1 to 3 SOM, respectively. From Tables 4 to 6, they are shown that the proposed method has 100% accuracy for the 150 training feature vectors in three SOMs.

Table 7 demonstrates the promising performance of Type 1 SOM when 300 testing patterns of three systems were tested. As shown in Table 7 among the 100 testing patterns of System 1, there are only two errors of recognition, one for VL, and the other for MH defects. The Table shows that among the 100 testing patterns of System 2, there is only one error of recognition for FH defect. It is shown in the Table that the proposed method has 100% accuracy for the 100 testing patterns of System 3. The test results give that Type 1 SOM is able to accurately recognize the testing defects for three systems. The number of features in the feature vector will influence the accuracy of pattern recognition. The best combination of feature vector for Type 1 SOM is System 3, the feature vector includes 14 features.

Table 8 demonstrates the promising performance of Type 2 SOM when 300 testing patterns of three systems were tested. As shown in Table 8 among the 100 testing patterns of System 1, there is only one error of recognition MH defects. The Table shows that among the 100 testing patterns of System 2, there is only one error of recognition for VH defect. The Table also displays that proposed method has 100% accuracy for the 100 testing patterns of System 3 and the Type 2 SOM is able to accurately recognize the testing defects for three systems. The best combination of feature vector for Type 2 SOM is System 3, the feature vector includes 14 features.

Table 9 demonstrates the promising performance of Type 3 SOM when 300 testing patterns of three systems were tested. As shown in Table 9 among the 100 testing patterns of System 1, there are only two errors of recognition, one for VH, and the other for MH defects. The Table shows that among the 100 testing patterns of System 2, there is only one error of recognition for FH defect. As shown in the Table, among the 100 testing patterns of System 3, only two errors of recognition exist, one for VH, and the other for MH defects. The best combination of feature vector for Type 3 SOM is System 2, the feature vector includes 12 features.

Table 4 Recognition performance of Type 1 SOM in training data (150 patterns)

System Pattern	Defect Types	Accuracy Rate
System 1 Training Data	NM	100%
	VH	100%
	VL	100%
	FH	100%
	MH	100%
System 2 Training Data	NM	100%
	VH	100%
	VL	100%
	FH	100%
	MH	100%
System 3 Training Data	NM	100%
	VH	100%
	VL	100%
	FH	100%
	MH	100%

Table 5 Recognition performance of Type 2 SOM in training data (150 patterns)

System Pattern	Defect Types	Accuracy Rate
System 1 Training Data	NM	100%
	VH	100%
	VL	100%
	FH	100%
	MH	100%
System 2 Training Data	NM	100%
	VH	100%
	VL	100%
	FH	100%
	MH	100%
System 3 Training Data	NM	100%
	VH	100%
	VL	100%
	FH	100%
	MH	100%

Table 6 Recognition performance of Type 3 SOM in training data (150 patterns)

System Pattern	Defect Types	Accuracy Rate
System 1 Training Data	NM	100%
	VH	100%
	VL	100%
	FH	100%
	MH	100%
System 2 Training Data	NM	100%
	VH	100%
	VL	100%
	FH	100%
	MH	100%
System 3 Training Data	NM	100%
	VH	100%
	VL	100%
	FH	100%
	MH	100%

Table 7 Recognition performance of Type 1 SOM in testing data (100 patterns)

System Pattern	Defect Types	Accuracy Rate
System 1 Testing Data	NM	100%
	VH	100%
	VL	95%
	FH	100%
	MH	95%
System 2 Testing Data	NM	100%
	VH	100%
	VL	100%
	FH	95%
	MH	100%
System 3 Testing Data	NM	100%
	VH	100%
	VL	100%
	FH	100%
	MH	100%

6 Conclusions

This paper has proposed an SOM based pattern recognition technique for PD of CRCTs. The effectiveness of the proposed technique has been verified using experimental results. It has been shown that through the feature extraction procedure, the extracted statistical featuring operators can significantly reduce the size of the PD pattern database. Also, the SOM based PD pattern recognition scheme is very effective for clustering the defects of CRCTs.

The experimental results show that the number of features in the feature vector influences the accuracy of pattern recognition. To further improve the recognition accuracy of the proposed approach, the optimal search methods, such as genetic programming and evolutionary programming, etc., for the best combination selection of feature vectors can be investigated and integrated in the proposed SOM based PD pattern recognition for the CRCTs and other high-voltage equipment. Besides, the structures of SOM have also been found to influence the accuracy of pattern recognition. To ameliorate further the recognition accuracy of the proposed approach, the optimized structure of the SOM can be studied in the future researches.

References:

[1] L. Niemeyer, A Generalized Approach to Partial Discharge Modeling, *IEEE Transactions on Dielectrics and Electrical Insulation*, Vol. 2, No. 4, August 1995, pp. 510-528**.**

[2] C. Cachin and H.J. Wiesmann, PD Recognition with Knowledge-Based Preprocessing and Neural Networks, *IEEE Transactions on Dielectrics and Electrical Insulation*, Vol. 2, No. 4, 1995, pp. 578-589**.**

[3] M.M.A. Salama and R. Bartnikas, Determination of Neural Network Topology for Partial Discharge Pulse Pattern Recognition, *IEEE Transactions on Neural Networks*, Vol. 13, No. 2, 2002, pp. 446-456.

[4] M.A. Bussab, J.I. Bernardo, and A. R. Hirakawa, Neural Networks Modeling in Greenhouse with Spatial Variability Identification, *WSEAS Transactions on Computer Research*, Volume 2, Issue 2, February 2007, pp. 214-219.

[5] M.H. Wang, Partial Discharge Pattern Recognition of Current Transformers Using an ENN, *IEEE Transactions on Power Delivery*, Vol. 20, No. 3, 2005, pp. 1984-1990.

[6] I. Oki, T. Haida, S. Wakabayashi, R. Tsuge, T. Sakakibarb, and H. Muraseg, Development of Partial Discharge Monitoring Technique Using a Neural Network in a Gas Insulated Substation, *IEEE Transactions on Power Systems*, Vol. 12, No. 2, May 1997, pp. 1014-1021.

[7] K. Zalis, Applications of Expert Systems in Evaluation of Data from Partial Discharge Diagnostic Measurement, *Proceedings of the 7th International Conference on Properties and Applications of Dielectric Materials*, 2003, pp. 331-334.

[8] M.S. Yang, W.L. Hung, and C.H. Chang, A Penalized Fuzzy Clustering Algorithm, *WSEAS Transactions on Computer Research*, Volume 1, Issue 2, December 2006, pp. 83-88.

[9] S.C. Wang and P.H. Huang, Fuzzy C-Means Clustering for Power System Coherency, *Proceedings of the 2005 IEEE International Conference on Systems, Man and Cybernetics*, 2005, pp. 2850-2855.

[10] W.Y. Chang and H.T. Yang, Application of Fuzzy C-Means Clustering Approach to Partial Discharge Pattern Recognition of Cast-Resin Current Transformers, *Proceedings of the 8th International Conference on Properties and Application of Dielectric Materials*, *ICPADM 2006*, Bali, Indonesia, 2006, pp. 372-375.

[11] J. Pi and M.F. Liao, Rolling Bearing Fault Diagnosis with Wavelet-Based Method, *WSEAS Transactions on Computer Research*, Volume 2, Issue 1, January 2007, pp. 1-7.

[12] Y. Zhang and L. Wu, Research on Time Series Modeling by Genetic Programming and Wavelet De-noising Performance of the Model, *WSEAS Transactions on Computer Research*, Volume 2, Issue 1, January 2007, pp. 44-49.

[13] Y. Tian, P.L. Lewin, S.J. Sutton, and S.G. Swingler, PD Characterization Using Wavelet Decomposition of Acoustic Emission Signals, *Proceedings of the 2004 International Conference on Solid Dielectrics*, Toulouse, France, July 5-9, 2004.

[14] Y. Tian, P.L. Lewin, A.E. Davies, S.G. Swingler, S.J. Sutton, and G.H. Hathaway, "Comparison of On-Line PD Detection Methods for High Voltage Cable Joints," *IEEE Transactions on Dielectrics and Electrical Insulation*, Vol. 9, No. 3, 2002, pp. 604-615.

[15] L. Satish and B. Nazneen, Wavelet-Based Denoising of Partial Discharge Signals Buried in Excessive Noise and Interference, *IEEE Transactions on Dielectrics and Electrical Insulation*, Vol. 10, No. 2, 2003, pp. 354-367.

Table 8 Recognition performance of Type 2 SOM in testing data (100 patterns)

System Pattern	Defect Types	Accuracy Rate
System 1 Testing Data	NM	100%
	VH	100%
	VL	100%
	FH	100%
	MH	95%
System 2 Testing Data	NM	100%
	VH	95%
	VL	100%
	FH	100%
	MH	100%
System 3 Testing Data	NM	100%
	VH	100%
	VL	100%
	FH	100%
	MH	100%

Table 9 Recognition performance of Type 3 SOM in testing data (100 patterns)

System Pattern	Defect Types	Accuracy Rate
System 1 Testing Data	NM	100%
	VH	95%
	VL	100%
	FH	100%
	MH	95%
System 2 Testing Data	NM	100%
	VH	100%
	VL	100%
	FH	95%
	MH	100%
System 3 Testing Data	NM	100%
	VH	95%
	VL	100%
	FH	100%
	MH	95%

[16] P. Wang, P.L. Lewin, Y. Tian, S.J. Sutton, and S.G. Swingler, Application of Wavelet-Based Denoising to Online Measurement of Partial Discharge, *Proceedings of the 2004 International Conference on Solid Dielectrics,* Toulouse, France, July 5-9, 2004.

[17] N.C. Sahoo and M.M.A. Salama, Trends in Partial Discharge Pattern Classification: A Survey, *IEEE Transactions on Dielectrics and Electrical Insulation*, Vol. 12, No. 2, 2005, pp. 248-264.

[18] Y. Han and Y.H. Song, Using Improved Self-organizing Map for Partial Discharge Diagnosis of Large Turbogenerators, *IEEE Transactions on Energy Conversion*, Vol. 18, No. 3, 2003, pp. 392-399.

[19] R.E. James and B.T. Phung, Development of Computer-based Measurements and Their Application to PD Pattern Analysis, *IEEE Transactions on Dielectrics and Electrical Insulation*, Vol. 2, No. 5, 1995, pp. 838-856.

[20] T. Lin, R.K. Aggarwal, and C.H. Kim, Identification of the Defective Equipments in GIS Using the Self Organising Map, *IEE Proc.- Generation Transmission Distribution*, Vol. 151, No. 5, 2004, pp. 644-650.

[21] Y. H. Song, H. B. Wan, and A. T. Johns, Power System Voltage Stability Assessment Using a Self-Organizing Neural Network Classifier, *Proceedings of the 4th International Conference on Power System Control and Management*, 1996, pp. 171–175.